Time Domain Acoustic Scattering from Underwater Elastic Objects Acquired through Fourier Synthesis Using COMSOL Multiphysics®

A. M. Gunderson*[1], B. E. Simon[1], A. L. Bonomo[1], and M. J. Isakson[1]

1. Applied Research Laboratories, University of Texas, Austin, TX, USA

* Corresponding author: 10000 Burnet Rd., Austin, TX 78758, aarong@@arlut.utexas.edu

Abstract: Finite element models for acoustic scattering from three dimensional underwater elastic objects, calculated in the frequency domain, are transformed to the time domain through Fourier synthesis using COMSOL Multiphysics®. The time domain mirrors the way in which experimental scattering data from real targets is acquired. Fluid elements are modeled using built-in physics in COMSOL's acoustics module, while elastic target elements are modeled with user-defined weak-form PDE interfaces. The problem is evaluated using a 2D axisymmetric geometry in COMSOL, and is extended to three dimensions through an axial wavenumber decomposition technique. Results show good agreement with established analytical solutions in both frequency and time domains.

Keywords: underwater acoustics, Fourier synthesis, acoustic scattering, time domain, axisymmetric.

I. Introduction

Of the various acoustic scattering studies on elastic targets, most published data-model comparisons appear in the frequency domain despite experimental data being naturally recorded in real time. Though the frequency domain comparison is informative, this precedent is also motivated by simplicity. Transformation of modeled data to the time domain requires fine frequency sampling to ensure a sufficiently long time window to capture elastic ringing, a requirement which can impose high computational demand. Typically it is simpler to record experimental data with a long time window, delivering high resolution frequency domain content for comparison.

The advantage of the time domain is the ability to isolate distinct scattered arrivals independently of each other, and to therefore match each arrival with a distinct scattering path, as in Ref. 1. Such arrivals often interfere in the frequency domain, making them impossible to isolate and identify. A high fidelity time domain model for elastic target scattering is therefore both highly desirable yet intensive to calculate. The finite element method (FEM) has been proven to be a robust method for predicting scatter from arbitrary objects with high fidelity and wide applicability. FEM results are rarely shown in the time domain, however, due to the high computational demand required to synthesize the scattering in 3D environments.

An efficient method of using FEM to model plane wave scattering from 3D axisymmetric targets, developed by Zampolli et. al.,[2] involves solving the problem using a 2D axisymmetric geometry and extending the results to three dimensions through an axial wavenumber decomposition (AWD) technique. In this method, the target is aligned with its axis of symmetry along the rotation axis of the 2D geometry, and the plane wave is incident at some angle ϕ relative to the r-axis, as shown in Fig. 1. Using cylindrical coordinates, the incident field $p_{inc}(r,\theta,z)$ is decomposed into a discrete azimuthal Fourier series:

$$p_{inc}(r,\theta,z) = \sum_{m=-\infty}^{\infty} [p_m(r,z)\exp(-im\theta)]. \qquad (1)$$

The component $p_m(r,z)$ is given by:

$$p_m(r,z) = (i^m)\exp(-ikz\sin\phi)J_m(-kr\cos\phi), \qquad (2)$$

where J_m designates the Bessel function of order m. The 3D problem may be solved by using the decomposed field components, given by Eq. (2), as incident fields in a series of 2D axisymmetric evaluations. The scattered field is then composed through a sum of Fourier components, analogous with Eq. (1). The convergence of the series with increasing $|m|$ in Eq. (1) allows for truncation of the sum at some maximum value m_{max}, with the value

$$m_{max} = 1.6k(\lambda_f + a)|\cos\phi| \qquad (3)$$

determined to be sufficiently large. In Eq. (3), k is the wavenumber and λ_f is the wavelength of the incident sound in the surrounding water, and a is a characteristic target dimension such as radius.

In this study, acoustic plane wave scattering from a variety of rigid and elastic targets in water was considered in the time domain. Plane waves were chosen as the incident pressure field to simulate the effect of a far field point source. Results were acquired through Fourier synthesis of FEM analysis
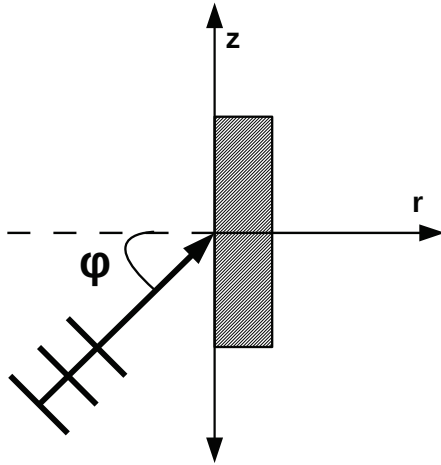
Figure 1. 2D axisymmetric geometry *(r,z)* used for AWD in COMSOL. The plane wave is incident at angle ϕ. In this geometry, a cylinder is represented as a rectangle which is spun about the *z*-axis.

at discrete frequencies using COMSOL Multiphysics and the LiveLink™ script for Matlab®. At each frequency step, the AWD technique of Zampolli et. al. was used to expedite the computation, allowing COMSOL to solve for the scattered field using a 2D axisymmetric geometry. Section II in this paper discusses how the geometry was divided into domains in COMSOL, and the governing equations and boundary conditions for each domain are given. Section III discusses the structure of the calculation, including how the AWD, frequency construction, and Fourier synthesis were implemented in COMSOL and LiveLink. Section IV displays time domain results for certain rigid and elastic targets. Results are compared to benchmark solutions to demonstrate the effectiveness of the method. Finally, concluding remarks are made in Section V.

II. Geometry, Governing Equations, and Boundary Conditions

For the FEM analysis in this study, the elements within the computational domain could be classified as belonging to (i) water, (ii) target material, or (iii) outer fluid domain. The target material could either be modeled as elastic or as rigid. Each class of domain had its own unique governing equations and boundary conditions imposed upon it.

The water surrounding the target was treated as a fluid, using the built-in Pressure Acoustics, Frequency Domain interface of COMSOL's Acoustics module. Within this interface, a typical density and sound speed for seawater were assumed:

ρ_f = 1000 kg/m^3 and c_f = 1500 m/s. Within the fluid domain, a background pressure field was applied to simulate the incident plane wave upon the target. An arbitrary angle of incidence ϕ was specified, and the field was constructed for a given axial wavenumber *m* according to Eq. (2).

Elastic target domains were evaluated through a user-input weak form PDE interface. As of version 5.2, COMSOL's built-in elastic domain interface does not allow for a nonzero axial wavenumber, and thus is inconsistent with AWD. Zampolli et. al. circumvented this problem by incorporating their own weak form PDE interface[2] for the elastic domains, which was also used in this study. This interface gave the volume integral portion of the weak form PDE in the "weak form PDE" node in COMSOL. The surface integral portion of the weak form PDE appeared in "Weak Contribution" nodes, along with fluid-elastic boundary conditions imposed at the edge of the target. For the elastic domain, it was sufficient to specify the density and the longitudinal and shear sound speeds in the material, and to calculate all other necessary elastic moduli from these inputs. This approach for treating elastic solids in COMSOL has previously been used in Ref. 2 and 3.

For rigid targets, the pressure field axiomatically was zero inside the target. Populating the inside of the target with elements thus became nonessential, and the exterior wall of the target could be made into a boundary of the computational domain. A rigid boundary condition was imposed, such that all incident waves were completely reflected.

The outermost portion of the fluid domain was modified to simulate an infinite domain by enforcing the Sommerfeld radiation condition. This was met by the placement of Bérenger Perfectly Matched Layers (PML's) over this domain. The PML is designed to absorb maximum energy from waves that are normal to the innermost PML boundary. Proper placement of the PML's could ensure all outward-going waves enter a PML at near-normal incidence, resulting in full absorption over the range of one wavelength. Thus, the PML was made to be the thickness of one wavelength, λ_f.

A free triangular mesh was imposed over the entire computational domain. The maximum element size was set to be $\lambda_f/6$, in accordance with the rule of thumb established by Bonomo and Isakson.[3] Thin boundary layers were also applied at the target-fluid boundary in order to create a very fine mesh where the field changed abruptly. These boundary layers were typically on the order of $\lambda_f/60$.

A far field calculation was evaluated using the solution at the PML inner boundary, through

COMSOL's built-in Far Field Calculation tool. The FEM calculation was evaluated in Matlab using the LiveLink script to import the model and results directly from COMSOL. Far-field results were imported directly into Matlab. Near-field results were interpolated onto a user defined grid of points in space, using LiveLink's "mphinterp" command.

III. AWD, Frequency Domain Construction, and Fourier Synthesis

Within COMSOL, an auxiliary sweep was applied to sample over axial wavenumber m from $-m_{max}$ to m_{max}. For field points in the r-z plane, $\theta = \{0, \pi\}$. Consequently, the evenness of the bracketed term in Eq. (1) allowed the sum to be restricted to the nonnegative m values, with the positive m terms multiplied by 2. For each element, COMSOL exported a list of scattered pressures corresponding to each m value. Matlab imported the data, interpolated the results onto the user-defined grid, and summed the scattered pressures for each m value to complete the AWD process.

An outer loop was then applied in Matlab to evaluate the model at different frequencies. Matlab looped over frequency and instructed COMSOL to reevaluate the model at each step. Frequency range and step size were variable, but were chosen to balance requirements for time domain duration and step size against computational time demand. The authors determined that the range of (dimensionless) frequencies $ka = 1\text{-}35$ provided sufficiently accurate time domain resolution through Fourier synthesis.

When all frequency domain results were evaluated, time domain results were obtained through Fourier synthesis using Matlab's inverse fast Fourier transform ("IFFT") command. This returned the scattering data displayed in time, with a uniquely defined time window. Time steps were determined by the relation $dt = 1/f_{max}$, where f_{max} was the highest frequency evaluated in the model. The time window spanned the space $t = 0$ to $t = t_{max}$, with $t_{max} = (N-1)dt$, and N was the number of points sampled.

IV. Results and comparison

Fig. 2 displays the near field backscattering from a 0.5 m diameter rigid sphere at a range of 1.5 m, evaluated through FEM in COMSOL and displayed on a decibel (dB) scale with variable frequency in (a). The result is then transformed to the time domain in (b) through Fourier synthesis. Also shown in Fig. 1 is the near-field backscattering partial wave series (PWS) solution for a rigid sphere, given by Morse and Ingard.[4] The two results show good

agreement in both frequency and time domains. Time domain results show two distinct arrivals corresponding to the initial specular reflection from the sphere, followed by the scattering of the circumnavigating Franz (creeping) wave on the sphere, as described by Rudgers.[5]
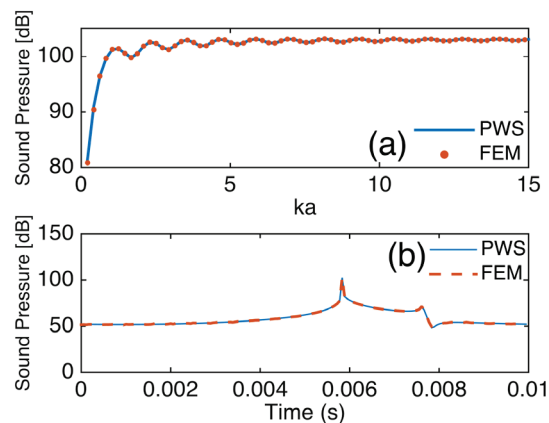

Figure 2. Backscattering from a rigid sphere, depicted in the (a) frequency and (b) time domains. FEM and PWS results are shown for comparison on a decibel scale.
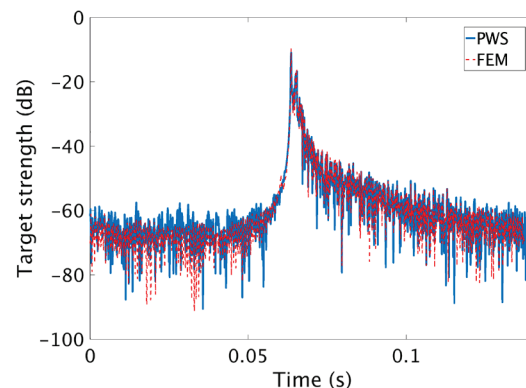

Figure 3. Time domain backscattering from an aluminum sphere, evaluated through FEM and PWS methods. Results are shown in terms of target strength.

Fig. 3 displays the far-field result for backscattering from an (elastic) aluminum sphere, with density $\rho = 2700$ kg/m^3, and longitudinal and shear sound speeds $c_L = 6176.4$ m/s and $c_T = 3103.2$ m/s. The incident plane wave was formed using AWD with $\phi = 90°$, corresponding to incidence in the positive z direction. The time domain FEM result was calculated at a point the backscattered direction, with coordinates (r,z) given in meters as $(0,-100)$. The result is shown in terms of target strength, given by $TS = 20log_{10}[r|p_{scat}(r,\theta,z)|/(r_0|p_{inc}(r,\theta,z)|)]$. Here, p_{scat} is the scattered pressure and $r_0 = 1$ m. The result is compared with the exact far-field partial wave series

solution for scattering from an elastic sphere, given by Marston.[6] The initial specular reflection is visible, followed by subsequent elastic arrivals which ring for an extended period of time.

To match the agreement between the solutions in Fig. 2 as closely as possible, the same incident waveform was used in both solutions, and was acquired as follows. First, the FEM time domain solution was evaluated at a point near the sphere in the near field. Then the incident wave pulse passing through this point was isolated in time, transformed to the frequency domain using a Fast Fourier Transform (FFT), and multiplied by the partial wave series solution. Finally, the result was transformed back to the time domain. This process is equivalent to a time domain convolution of the incident signal with the target's impulse response function, and mirrors the approach used for time domain scattering results in Ref. 1, 5, and 7.
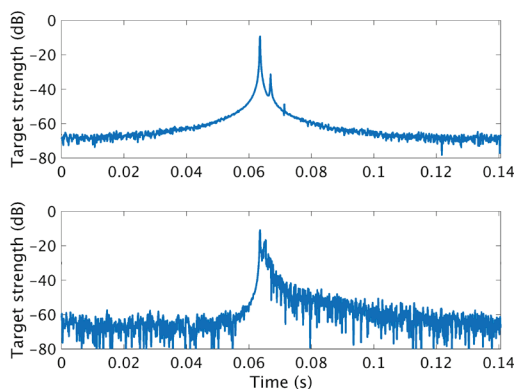

Figure 4. Time domain backscattering from a (a) rigid and (b) aluminum sphere. Results are shown in terms of target strength.

Fig. 4 displays the far-field FEM time domain backscattering results for the one meter radius rigid and aluminum spheres at $(r,z) = (0,-100)$, when a plane wave was incident at $\phi = 90°$. The earliest arrival in both solutions, the specular reflection, arrives simultaneously. It is higher amplitude for the rigid sphere, due to the rigid sphere's larger reflection coefficient. Subsequent elastic ringing is visible for the aluminum sphere solution. The Franz arrival is distinctly visible for the rigid sphere, but is likely too small to be observed amidst the larger amplitude elastic behavior in the aluminum sphere solution.

Fig. 5 displays the far-field backscattering result for a 4:1 length-to-diameter ratio steel cylinder, with a plane wave incident broadside. The steel material parameters were $\rho = 7800$ kg/m^3, $c_L = 5800$ m/s, and $c_T = 3200$ m/s. The result is displayed in terms of target strength. The time domain FEM result is compared to a far field approximate PWS solution

given by Stanton.[8] The two results have much in common, including an initial specular reflection followed by distinct subsequent elastic arrivals, which ring for an extended time duration. Stanton's model neglects contributions from the cylinder endcaps, though these contribute minimally for broadside scattering. At broadside, however, $\phi = 0°$ and m_{max} is maximized, requiring computation of a large number of terms to go into the axial wavenumber sum. Small-scale differences between the two solutions in Fig. 5 are more likely due to truncation of this sum, or the inclusion of too few frequencies, than they are to limitations of Stanton's solution. Agreement is strong above $TS = -30$ dB.
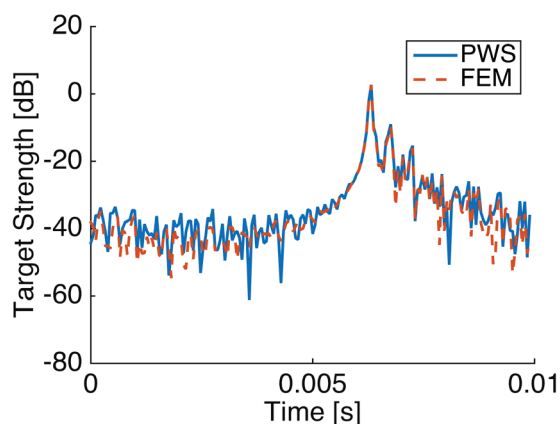

Figure 5. Time domain backscattering from a 4:1 steel cylinder, incident broadside. FEM and PWS results are shown in terms of target strength for comparison.

V. Conclusions

The results in Sec. IV have verified the ability of Fourier synthesized FEM results to capture the time domain scattering behavior of elastic targets. The utility of this method merits further discussion here. When comparing FEM and partial wave series solutions, construction of the FEM frequency domain content takes considerably longer to evaluate. However, the wide applicability of the FEM solution is its appeal. Exact, or even approximate, scattering solutions are frequently not known for certain classes of targets, or even for simple targets at certain orientations or in certain environments. Additionally, near-field scattering solutions for elastic targets are rarely known.

Fourier synthesis of FEM results is therefore the closest thing to a solution for scattering from complicated targets and geometries for which exact solutions are not available. Assuming the Sommerfeld radiation condition is satisfied through proper PML placement, the error associated with the synthesized FEM solution is determined by the size

of the mesh, and the step sizes and lengths of the axial wavenumber and frequency sampling ranges: all controllable parameters within the FEM-Fourier synthesis framework. The AWD technique of Zampolli et. al. trims the computational time demand enough that Fourier synthesis of FEM solutions can be computed on manageable time scales. This time reduction makes the FEM-Fourier synthesis combination an appealing candidate for providing time domain scattering models for any variety of elastic target.

VI. Acknowledgements

References

1. A.M. Gunderson and P.L. Marston, "Kirchhoff approximation for backscattering from a partially exposed rigid sphere at a flat interface," *J. Acoust. Soc. Am.*, **140**, 3582-3592 (2016).
2. M. Zampolli, A. Tesei, F.B. Jensen, N. Malm, and J.B. Blottman III, "A computationally efficient finite element model with perfectly matched layers applied to scattering from axially symmetric objects," *J. Acoust. Soc Am.,* **122**, 1472-1485 (2007).
3. A.L. Bonomo and M.J. Isakson, "Modeling the acoustic scattering from axially symmetric fluid, elastic, and poroelastic objects due to nonsymmetric forcing using COMSOL Multiphysics," Proc. COMSOL Conf. in Boston, (2016).
4. P.M. Morse and K.U. Ingard, *Theoretical Acoustics*, 418-419. Princeton Univ. Press, Princeton, NJ (1968).
5. A.J. Rudgers, "Acoustic pulses scattered by a rigid sphere immersed in a fluid," *J. Acoust. Soc. Am.*, **45**, 900-910 (1969).
6. P.L. Marston, "Acoustic beam scattering and excitation of sphere resonance: Bessel beam example", *J. Acoust. Soc. Am.*, **122**, 247-252 (2007).
7. L.G. Zhang, N.H. Sun, and P.L. Marston, "Midfrequency enhancement of the backscattering of tone bursts by thin spherical shells," *J. Acoust. Soc. Am.*, **91**, 1862-1874 (1992).
8. T.K. Stanton, "Sound scattering by cylinders of finite length. II. Elastic cylinders," *J. Acoust. Soc. Am.*, **83**, 64-67 (1988).